Physics Letters B 681 (2009) 418–422

Contents lists available at ScienceDirect

Physics Letters B

www.elsevier.com/locate/physletb

Nearly perfect fluid in Au + Au collisions at RHIC

A.K. Chaudhuri

Variable Energy Cyclotron Centre, 1/AF, Bidhan Nagar, Kolkata 700 064, India

ARTICLE INFO

Article history:
Received 3 September 2009
Received in revised form 8 October 2009
Accepted 21 October 2009
Available online 24 October 2009
Editor: J.-P. Blaizot

PACS:
47.75.+f
25.75.-q
25.75.Ld

ABSTRACT

In the Israel–Stewart's theory of dissipative hydrodynamics, we have analysed the STAR data on ϕ meson production in Au+Au collisions at $\sqrt{s} = 200$ GeV. From a simultaneous fit to ϕ mesons multiplicity, mean p_T and integrated v_2, we obtain a phenomenological estimate of QGP viscosity, $\eta/s = 0.07 \pm 0.03 \pm 0.14$, the first error is due to the experimental uncertainty in STAR measurements, the second reflects the uncertainties in initial and final conditions of the fluid.

In recent years, there has been considerable interest in viscosity of strongly interacting Quark–Gluon Plasma. String theory based models (ADS/CFT) give a lower bound on viscosity of any matter $\eta/s \geqslant 1/4\pi$ [1]. In a perturbative QCD, Arnold et al. [2] estimated $\eta/s \sim 1$. In a SU(3) gauge theory, Meyer [3] gave the upper bound $\eta/s < 1.0$, and his best estimate is $\eta/s = 0.134(33)$ at $T = 1.165T_c$. At RHIC region, Nakamura and Sakai [4] estimated the viscosity of a hot gluon gas as $\eta/s = 0.1$–0.4. Attempts have been made to estimate QGP viscosity directly from experimental data. Gavin and Abdel-Aziz [5] proposed to measure viscosity from transverse momentum fluctuations. From the existing data on Au + Au collisions, they estimated that QGP viscosity as $\eta/s = 0.08$–0.30. Experimental data on elliptic flow has also been used to estimate QGP viscosity. Elliptic flow scales with eccentricity. Departure form the scaling can be understood as due to off-equilibrium effect and utilised to estimate viscosity [6] as, $\eta/s = 0.11$–0.19. Experimental observation that elliptic flow scales with transverse kinetic energy is also used to estimate QGP viscosity, $\eta/s \sim 0.09 \pm 0.015$ [7], a value close to the ADS/CFT bound. From heavy quark energy loss, PHENIX Collaboration [8] estimated QGP viscosity $\eta/s \approx 0.1$–0.16. Recently, from analysis of RHIC data, in a viscous hydrodynamics, upper bound to viscosity is given $\eta/s < 0.5$ [9,10].

In the present Letter, from a hydrodynamic analysis of the recently measured STAR data [11] on ϕ production, we have obtained an accurate estimate of QGP viscosity, $\eta/s = 0.07 \pm 0.03 \pm 0.14$, the first error corresponding the uncertainty in STAR measurements, the 2nd error arising from the uncertain initial conditions of the fluid, e.g. initial time, initial fluid velocity, freeze-out temperature, etc. As noted in [12], several unique features of ϕ mesons (e.g. hidden strange particle, both hadronic and leptonic decays, not affected by resonance decays, mass and width are not modified in a medium [13], etc.) make it an ideal probe to investigate medium properties in heavy ion collisions. For long, strangeness enhancement is considered as a signature of QGP formation [14]. Compared to a hadron gas, in QGP, strangeness is enhanced due to abundant $gg \to s\bar{s}$ reactions. Early produced $s\bar{s}$, if survives hadronisation can lead to increased production of strange particles compared to pp or pA collisions. Experimental data do show strangeness enhancement [15]. In STAR measurements [11] also, compared to a pp collision, in an Au + Au collision, ϕ meson production is enhanced. STAR data [11] also appear to be consistent with a model based on recombination of thermal strange quarks [16]. As it will be shown below, STAR data on ϕ mesons are also consistent with hydrodynamic model and are sensitive enough to give an accurate estimate of QGP viscosity.

Space–time evolution of the QGP fluid is obtained by solving, Israel–Stewart's theory of 2nd order dissipative hydrodynamics.

$$\partial_\mu T^{\mu\nu} = 0, \tag{1}$$

$$D\pi^{\mu\nu} = -\frac{1}{\tau_\pi}\left(\pi^{\mu\nu} - 2\eta\nabla^{\langle\mu}u^{\nu\rangle}\right) - \left[u^\mu\pi^{\nu\lambda} + u^\nu\pi^{\nu\lambda}\right]Du_\lambda. \tag{2}$$

Eq. (1) is the conservation equation for the energy–momentum tensor, $T^{\mu\nu} = (\varepsilon + p)u^\mu u^\nu - pg^{\mu\nu} + \pi^{\mu\nu}$, ε, p and u being the energy density, pressure and fluid velocity, respectively. $\pi^{\mu\nu}$ is the shear stress tensor (we have neglected bulk viscosity and heat conduction). Eq. (2) is the relaxation equation for the shear stress tensor $\pi^{\mu\nu}$. In Eq. (2), $D = u^\mu\partial_\mu$ is the convective time derivative, $\nabla^{\langle\mu}u^{\nu\rangle} = \frac{1}{2}(\nabla^\mu u^\nu + \nabla^\nu u^\mu) - \frac{1}{3}(\partial\,.\,u)(g^{\mu\nu} - u^\mu u^\nu)$ is a symmetric

E-mail address: akc@veccal.ernet.in.

0370-2693
doi:10.1016/j.physletb.2009.10.068

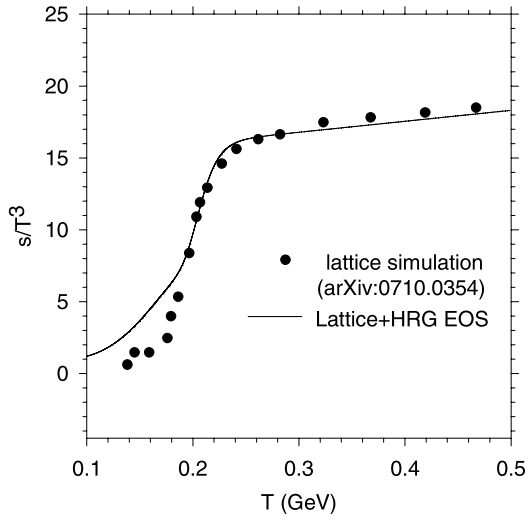

Fig. 1. Black circles are lattice simulation [19] for entropy density. The black line is the model EOS, obtained by parametric representation to the lattice simulations and a hadronic resonance gas at low temperature.

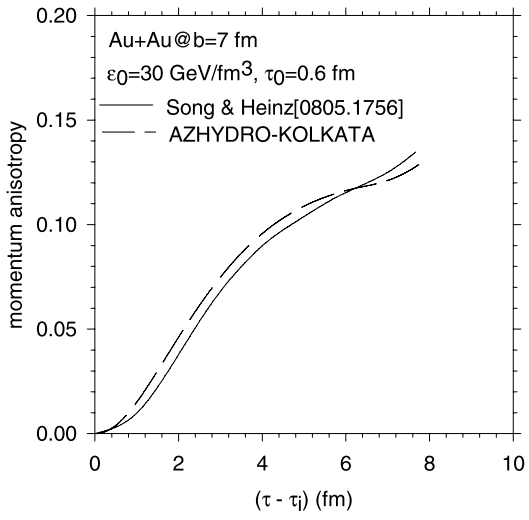

Fig. 2. Viscous fluid ($\eta/s = 0.08$) simulation for temporal evolution of momentum anisotropy in $b = 7$ fm Au+Au collision at RHIC. The solid line is the simulation result from VISH2 + 1 [17] and the dashed line is the simulation result from AZHYDRO–KOLKATA.

traceless tensor. η is the shear viscosity and τ_π is the relaxation time. It may be mentioned that in a conformally symmetric fluid relaxation equation can contain additional terms [17].

Eqs. (1), (2) are closed with an equation of state $p = p(\varepsilon)$. Lattice simulations [18,19] indicate that the confinement–deconfinement transition is a cross over, rather than a 1st or 2nd order phase transition. In Fig. 1, a recent lattice simulation [19] for the entropy density is shown. We complement the lattice simulated EOS [19] by a hadronic resonance gas (HRG) EOS comprising all the resonances below mass 2.5 GeV. In Fig. 2, the solid line is the entropy density of the "lattice + HRG" EOS. The entropy density is obtained as

$$s = 0.5\big[1 - \tanh(x)\big]s_{HRG} + 0.5\big[1 - \tanh(x)\big]s_{lattice} \tag{3}$$

with $x = \frac{T-T_c}{\Delta T}$, $T_c = 196$ MeV, $\Delta T = 0.1T_c = 19.6$ MeV. Compared to lattice simulation, entropy density drops slowly at low temperature.

Assuming boost-invariance, Eqs. (1) and (2) are solved in ($\tau = \sqrt{t^2 - z^2}, x, y, \eta_s = \frac{1}{2}\ln\frac{t+z}{t-z}$) coordinates, with a code "AZHYDRO–KOLKATA", developed at the Cyclotron Centre, Kolkata. Details of the code can be found in [21]. To show that AZHYDRO–KOLKATA computes the evolution correctly, in Fig. 1, we have compared the temporal evolution of momentum anisotropy $\varepsilon_p = \frac{\langle T^{xx} - T^{yy}\rangle}{\langle T^{xx} + T^{yy}\rangle}$ of a QGP fluid with a calculation of Song and Heinz [17]. Initial conditions are approximately same in both simulations. Within 10% or less, AZHYDRO–KOLKATA simulation reproduces Song and Heinz's [17] result for temporal evolution of momentum anisotropy ε_p.

Solution of partial differential equations (Eqs. (1), (2)) requires initial conditions, e.g. transverse profile of the energy density ($\varepsilon(x, y)$), fluid velocity ($v_x(x, y), v_y(x, y)$) and shear stress tensor ($\pi^{\mu\nu}(x, y)$) at the initial time τ_i. One also needs to specify the viscosity (η) and the relaxation time (τ_π). A freeze-out prescription is also needed to convert the information about fluid energy density and velocity to particle spectra and compare with experiment.

We assumed that the fluid is thermalised at $\tau_i = 0.6$ fm [20] and the initial fluid velocity is zero, $v_x(x, y) = v_y(x, y) = 0$. Initial energy density is assumed to be distributed as [20]

$$\varepsilon(\mathbf{b}, x, y) = \varepsilon_i\big[0.75N_{part}(\mathbf{b}, x, y) + 0.25N_{coll}(\mathbf{b}, x, y)\big], \tag{4}$$

where b is the impact parameter of the collision. N_{part} and N_{coll} are the transverse profile of the average number of participants and average number collisions, respectively. ε_i is a parameter which does not depend on the impact parameter of the collision. As will be discussed below, we fix it to reproduce experimental data on ϕ mesons. Finally, the freeze-out was fixed at $T_F = 150$ MeV.[1] The shear stress tensor was initialised with boost-invariant value, $\pi^{xx} = \pi^{yy} = 2\eta/3\tau_i$, $\pi^{xy} = 0$. For the relaxation time, we used the Boltzmann estimate $\tau_\pi = 3\eta/2p$.

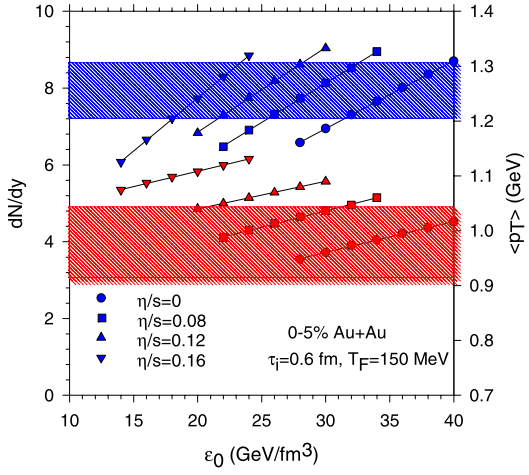

Fig. 3. (Color online.) Variation of $\frac{dN^\phi}{dy}$ and $\langle p_T^\phi\rangle$ with central energy density in $b = 2.3$ fm Au + Au collisions in AZHYDRO–KOLKATA. The blue and red symbols are the predicted $\frac{dN^\phi}{dy}$ and $\langle p_T^\phi\rangle$ respectively for $\eta/s = 0.0$, 0.08, 0.16, 0.2 and 0.25. The blue and red shaded regions indicate the STAR measurements (statistical and systematic error included) of $\frac{dN^\phi}{dy}$ and $\langle p_T^\phi\rangle$ in 0–5% centrality Au + Au collisions.

In Fig. 3, for fluid viscosity, $\eta/s = 0$, 0.08, 0.12 and 0.16, hydrodynamic predictions for ϕ meson multiplicity ($\frac{dN^\phi}{dy}$) and mean p_T ($\langle p_T^\phi\rangle$), in $b = 2.3$ fm Au + Au collisions are shown as a function of central energy density. In a hydrodynamic model, as expected, both $\frac{dN^\phi}{dy}$ and $\langle p_T^\phi\rangle$ increase with increasing energy density, but

[1] We have checked that with the lattice + HRG EOS, in ideal fluid dynamics, STAR measurements of $\frac{dN^\phi}{dy}$ and $\langle p_T^\phi\rangle$ in 0–5% Au + Au collisions are best explained with $T_F = 150$ MeV.

Table 1
The fitted values of the initial central energy density (ε_i) and temperature (T_i) of the fluid in $b = 0$ Au + Au collisions, for different values of viscosity to entropy ratio (η/s). In the last four rows, χ^2/N for STAR data on $\frac{dN^\phi}{dy}$, $\langle p_T^\phi \rangle$, v_2 and the combined data sets ($\frac{dN^\phi}{dy} + \langle p_T^\phi \rangle + v_2$) are shown.

η/s	0	0.08	0.12	0.16
ε_i (GeV/fm^3)	35.5	29.1	25.6	20.8
	±5.0	±3.6	±4.0	±2.7
T_i (MeV)	377.0	359.1	348.0	330.5
	±13.7	±11.5	±14.3	±11.3
χ^2/N (dN/dy)	4.3	4.5	3.9	2.21
χ^2/N ($\langle p_T \rangle$)	0.55	0.26	1.80	6.22
χ^2/N (v_2)	4.92	2.99	2.79	3.03
χ^2/N ($dN/dy + \langle p_T \rangle + v_2$)	9.77	7.76	8.49	11.46

increase in $\frac{dN^\phi}{dy}$ is steeper than in $\langle p_T^\phi \rangle$. $b = 2.3$ fm Au + Au collisions correspond to 0–5% centrality collisions. In Fig. 3, the blue and red shaded regions represent the STAR measurements (statistical and systematic error included) on ϕ mesons multiplicity and mean p_T in 0–5% Au + Au collisions. One notes that irrespective of fluid viscosity, ϕ meson multiplicity can be fitted in the hydrodynamic model by changing the initial energy density, more viscous fluid requiring less energy density. It is understood. In viscous fluid evolution, entropy is generated and fluid requires less initial entropy density or energy density. However, with increasing η/s, mean p_T also increases, even if ϕ meson multiplicity is kept fixed by reducing initial energy density. The reason is understood. Initial transverse pressure increases with increasing η/s leading to increased $\langle p_T \rangle$. One notes that simultaneous fit to STAR data on ϕ multiplicity and mean p_T in 0–5% centrality Au + Au collisions is obtained only when $\eta/s \leqslant 0.12$. For higher viscosity, while it is possible to fit ϕ meson multiplicity, mean p_T is overpredicted.

In Fig. 4, in three panels, STAR data [11] on the centrality dependence of ϕ meson (a) multiplicity ($\frac{dN^\phi}{dy}$), (b) integrated v_2 and (c) mean p_T ($\langle p_T^\phi \rangle$) are shown. Ideal or viscous fluid, initialised to fit ϕ meson multiplicity in 0–5% collisions, reproduces ϕ meson multiplicity in all the centrality ranges of collisions. STAR Collaboration measured integrated v_2 only in 0–5%, 10–40% and 40–80% centrality collisions. In mid-central collisions, v_2 is reduced by $\sim 10\%$. In very central collisions, elliptic flow is very small and ideal and viscous evolutions produce similar flow. In peripheral collisions, both ideal and viscous evolutions overestimate the flow. We also observe that the STAR data on $\langle p_T^\phi \rangle$ are not explained unless $\eta/s \leqslant 0.12$, as indicated in Fig. 4.

In Table 1, we have tabulated the initial central energy density (ε_i) and temperature (T_i) required to fit the STAR data on ϕ multiplicity. The error in ε_i is due to the statistical + systematic error in STAR measurement. The initial energy density of the fluid can be obtained only within ~ 10–15% accuracy. In Table 1, we have listed the χ^2/N for the data sets analysed. Variation of χ^2/N of the combined data sets with η/s, is shown in Fig. 5. In Fig. 5, the solid line is a parabolic fit to the combined χ^2/N, from which we estimate that the best fit to the STAR data on the centrality dependence of ϕ mesons multiplicity, integrated v_2 and mean p_T are obtained for viscosity over entropy ratio as $\eta/s = 0.07 \pm 0.03$. We have not shown here, but hydrodynamics with $\eta/s \approx 0.07$ consistently explain transverse momentum spectra of ϕ mesons, along with other particles, e.g. pions, kaons. Interestingly, proton data is underestimated in the model by a factor of 2. Elliptic flow data are also reasonably well explained. In a later publication detailed results will be presented.

The estimate $\eta/s = 0.07 \pm 0.03$ is obtained with fixed values of initial time $\tau_i = 0.6$ fm, freeze-out temperature $T_F = 150$ MeV, and initial transverse velocity $v_r = 0$. The hard scattering contribution to initial energy density was also fixed at 25%. The estimate depends on the assumed initial and final conditions of the fluid. In Fig. 6, we have studied the dependence of $\frac{dN^\phi}{dy}$ and $\langle p_T^\phi \rangle$ on: (a) initial time, (b) freeze-out temperature, (c) hard scattering contribution to initial energy density and (d) initial transverse velocity. The fluid was initialised with central energy density $\varepsilon_i = 29.1$ GeV/fm^3, corresponding to viscosity to entropy ratio $\eta/s = 0.08$. Other conditions remaining the same, hydrodynamic predictions for $\frac{dN^\phi}{dy}$ and $\langle p_T^\phi \rangle$ increase respectively by $\sim 50\%$ and $\sim 10\%$ as τ_i increases from 0.6 fm to 1.0 fm. If τ_i is reduced from 0.6 to 0.2 fm, $\frac{dN^\phi}{dy}$ decreases by $\sim 50\%$, $\langle p_T^\phi \rangle$ remains essentially unchanged. For $\tau_i = 1$ fm, STAR data on ϕ multiplicity can be reproduced if initial energy density of the fluid is reduced by $\sim 40\%$ (we are assuming that $\frac{dN^\phi}{dy}$ dependence of initial energy density is similar at $\tau_i = 0.6$ and 1 fm). However, $\sim 40\%$ reduction in energy density will also reduce $\langle p_T^\phi \rangle$ by $\sim 7\%$ ($\langle p_T^\phi \rangle$ dependence on initial energy density is weaker than that of $\frac{dN^\phi}{dy}$) and STAR data on $\langle p_T^\phi \rangle$ will be overpredicted by $\sim 3\%$, requiring $\sim 55\%$ less viscosity. Arguing similarly, for $\tau_i = 0.2$ fm, to fit ϕ multiplicity, initial energy density is to be increased by $\sim 40\%$, which will also increase $\langle p_T^\phi \rangle$ by $\sim 7\%$, requiring $\sim 90\%$ reduction in η/s. We estimate systematic uncertainty in η/s due to uncertain initial time ($\tau_i = 0.6 \pm 0.4$ fm) as $\sim 90\%$.

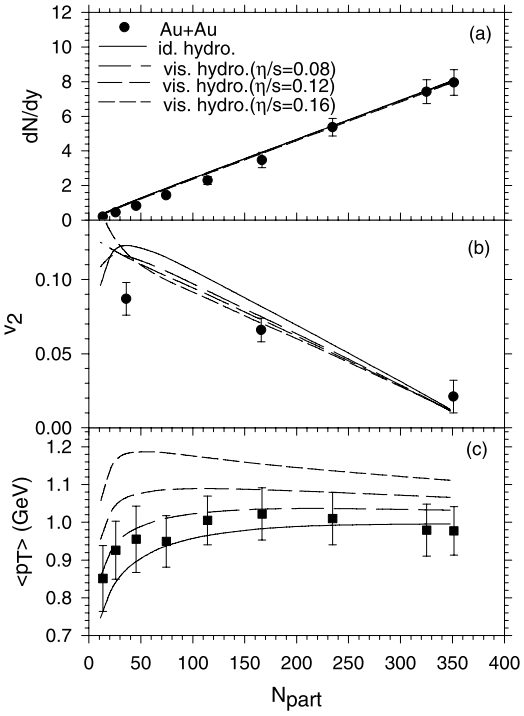

Fig. 4. STAR data on the centrality dependence of ϕ meson (a) multiplicity, (b) integrated v_2 and (c) mean p_T are compared with hydrodynamical simulation of ideal and viscous fluid.

One of the major sources of uncertainty in hydrodynamic simulations is the freeze-out temperature (T_F). If T_F is increased from 150 to 160 MeV, hydrodynamic prediction overestimates the STAR data for $\frac{dN^\phi}{dy}$ by 15%, $\langle p_T^\phi \rangle$ remains essentially unchanged (see Fig. 4b). Initial energy density of the fluid can be reduced by $\sim 10\%$ to fit ϕ multiplicity, which will simultaneously reduce $\langle p_T^\phi \rangle$ by $\sim 2\%$. $\sim 2\%$ reduction in $\langle p_T^\phi \rangle$ can be compensated by increasing η/s by $\sim 7\%$. If T_F decreases from 150 to 140 MeV, hydrodynamic prediction for $\frac{dN^\phi}{dy}$ underestimates the STAR data by $\sim 15\%$ and

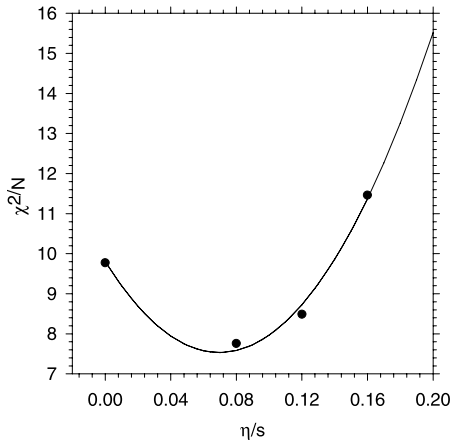

Fig. 5. Variation of χ^2/N of the combined data sets with η/s. The solid line is a parabolic fit to χ^2/N.

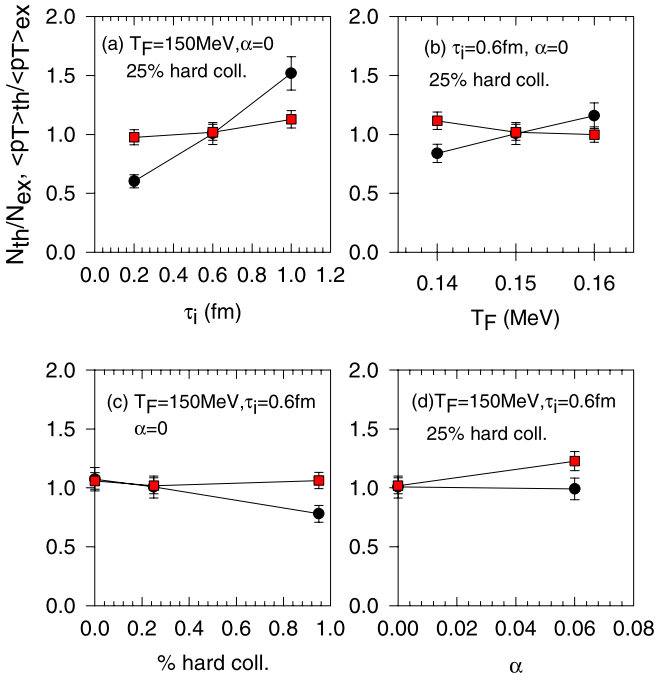

Fig. 6. (Color online.) The ratio of hydrodynamic predictions for $\frac{dN^\phi}{dy}$ (the black circles) and $\langle p_T^\phi \rangle$ (the red squares), to STAR measurements in 0–5% Au + Au collisions as a function of (a) initial time (τ_i), (b) freeze-out temperature (T_F), (c) hard scattering contribution to initial energy density, and (d) initial transverse velocity ($v_r = \tanh(\alpha r)$), are shown. The central energy density of the fluid is $\varepsilon_i = 29.1$ GeV/fm^3 and viscosity to entropy ratio is $\eta/s = 0.08$.

overestimates $\langle p_T^\phi \rangle$ by $\sim 10\%$. Initial energy density can be increased by $\sim 10\%$ to fit $\frac{dN^\phi}{dy}$, which will increase $\langle p_T^\phi \rangle$ by $\sim 2\%$. $\sim 12\%$ increase in $\langle p_T^\phi \rangle$ cannot be compensated by decreasing η/s and $T_F = 140$ MeV will be inconsistent with STAR measurements. Indeed, even in ideal hydrodynamics, $T_F = 140$ MeV overpredicts STAR data on $\langle p_T^\phi \rangle$. We estimate the uncertainty in η/s due to uncertain freeze-out temperature ($T_F = 150 \pm 10$ MeV) as $\sim 100\%$.

In Fig. 6c, dependence of $\frac{dN^\phi}{dy}$ and $\langle p_T^\phi \rangle$ on the hard scattering contribution to initial energy density is studied. If hard scattering contribution is increased from 25% to 95%, hydrodynamic predictions for $\frac{dN^\phi}{dy}$ decrease by $\sim 20\%$, but $\langle p_T^\phi \rangle$ remains essentially unchanged. As argued previously, to fit the STAR data on ϕ multiplicity, initial energy density is to be increased by $\sim 15\%$, which will lead to increase of $\langle p_T^\phi \rangle$ by $\sim 3\%$. $\sim 3\%$ increase in p_T can be compensated by reducing η/s by $\sim 55\%$. If hard scattering contribution decreases from 25% to 5%, predicted $\frac{dN^\phi}{dy}$ and $\langle p_T^\phi \rangle$ change marginally and estimate of η/s will not be affected. We estimate the uncertainty in η/s due to uncertain hard scattering contribution (0–100%) as $\sim 55\%$.

Hydrodynamic predictions for $\frac{dN^\phi}{dy}$ and $\langle p_T^\phi \rangle$ as a function of the initial transverse velocity $v_r = \tanh(\alpha r)$, for $\alpha = 0$, and 0.06 are shown in Fig. 6d. Initial transverse velocity mainly increases high p_T yield and as α increases from 0 to 0.06, $\frac{dN^\phi}{dy}$ remains approximately constant, but $\langle p_T^\phi \rangle$ increases and the STAR measurement for $\langle p_T \rangle$ is overpredicted by $\sim 20\%$. Indeed, non-zero initial transverse velocity will increase $\langle p_T^\phi \rangle$ requiring lowering of η/s. We then estimate uncertainty in η/s due to uncertain initial velocity as $\sim 100\%$. Finite accuracy in the computer code AZHYDRO–KOLKATA also adds to the uncertainty in η/s. In AZHYDRO–KOLKATA, hydrodynamic evolution is computed within $\sim 5\%$ accuracy, leading to the $\sim 7\%$ uncertainty in η/s. Adding all the uncertainties is quadrature, systematic uncertainty in η/s is $\sim 175\%$. From the STAR data on ϕ meson we then estimate QGP viscosity as $\eta/s = 0.07 \pm 0.03 \pm 0.14$, the first uncertainty is due to statistical and systematic uncertainty in STAR measurements, the second one is due to uncertain initial time ($\tau_i = 0.2$–1.0 fm), freeze-out temperature ($T_F = 140$–160 MeV), percentage of hard scattering contribution ($f = 0$–95%) and initial transverse velocity ($\alpha = 0$–0.6).

It may be noted that the sources of uncertainties considered here is not exhaustive. For example, the uncertainty in the initial energy density may not be represented in entirety by the Glauber model, by varying only the hard scattering fraction. Color Glass Condensate initial conditions, with larger initial eccentricity, may increase the range of η/s. The uncertainty in freeze-out procedure is also not entirely represented by varying freeze-out temperature only. Proper treatment of chemical freeze-out before the kinetic freeze-out, inclusion of resonances may also alter the range of uncertainty in η/s. Also, as mentioned earlier, the relaxation equation (2), may contain additional terms. While their contribution is expected to be smaller than the terms included, estimate of viscosity may change if a more complete relaxation equation is used. Uncertainty in the initial shear stress tensor is also not considered here. We have used boost-invariant value as the initial shear stress tensor. While over the time scale τ_π, Israel–Stewart stress relaxes to the first order value, i.e. to the boost invariant value, it may as well be different at the initial time. Range of uncertainty in η/s will also increase if uncertainty in initial shear stress tensor is taken into consideration.

The estimate is obtained from experimental data, which include the effect of bulk viscosity, if there is any. We have neglected bulk viscosity. Neglect of bulk viscosity will artificially increase the effect of (shear) viscosity. In general, bulk viscosity is an order of magnitude smaller than shear viscosity. But in QGP, it is possible that near the cross-over temperature, bulk viscosity is large [22,23]. Effect of bulk viscosity on particle spectra and elliptic flow is studied in [24]. It appears that even if small, bulk viscosity can have visible effect on particle spectra and elliptic flow. The present estimate then must be considered as an upper bound on QGP viscosity.

References

[1] G. Policastro, D.T. Son, A.O. Starinets, Phys. Rev. Lett. 87 (2001) 081601.
[2] P. Arnold, G.D. Moore, L.G. Yaffe, JHEP 0011 (2000) 001;
P. Arnold, G.D. Moore, L.G. Yaffe, JHEP 0305 (2003) 051.

[3] H.B. Meyer, Phys. Rev. D 76 (2007) 101701, arXiv:0704.1801 [hep-lat].
[4] A. Nakamura, S. Sakai, Nucl. Phys. A 774 (2006) 775.
[5] S. Gavin, M. Abdel-Aziz, Phys. Rev. Lett. 97 (2006) 162302, arXiv:nucl-th/0606061.
[6] H.J. Drescher, A. Dumitru, C. Gombeaud, J.Y. Ollitrault, Phys. Rev. C 76 (2007) 024905, arXiv:0704.3553 [nucl-th].
[7] R.A. Lacey, et al., Phys. Rev. Lett. 98 (2007) 092301, arXiv:nucl-ex/0609025.
[8] A. Adare, et al., PHENIX Collaboration, Phys. Rev. Lett. 98 (2007) 172301, arXiv:nucl-ex/0611018.
[9] M. Luzum, P. Romatschke, Phys. Rev. C 78 (2008) 034915, arXiv:0804.4015 [nucl-th].
[10] H. Song, U.W. Heinz, arXiv:0812.4274 [nucl-th].
[11] B.I. Abelev, et al., STAR Collaboration, Phys. Rev. Lett. 99 (2007) 112301, arXiv:nucl-ex/0703033.
[12] B. Mohanty, N. Xu, arXiv:0901.0313 [nucl-ex].
[13] C. Alt, et al., NA49 Collaboration, Phys. Rev. C 78 (2008) 044907, arXiv:0806.1937 [nucl-ex].
[14] P. Koch, B. Muller, J. Rafelski, Phys. Rep. 142 (1986) 167.
[15] J.H. Chen, for the STAR Collaboration, J. Phys. G: Nucl. Part. Phys. 35 (2008) 104053.
[16] R.C. Hwa, C.B. Yang, arXiv:nucl-th/0602024.
[17] H. Song, U.W. Heinz, Phys. Rev. C 78 (2008) 024902, arXiv:0805.1756 [nucl-th].
[18] F. Karsch, E. Laermann, P. Petreczky, S. Stickan, I. Wetzorke, in: H. Rollnik, D. Wolf (Eds.), Proceedings of NIC Symposium, 2001, NIC Series, vol. 9, John von Neumann Institute for Computing, Jülich, ISBN 3-00-009055-X, 2002, pp. 173–182.
[19] M. Cheng, et al., Phys. Rev. D 77 (2008) 014511, arXiv:0710.0354 [hep-lat].
[20] P.F. Kolb, U. Heinz, in: R.C. Hwa, X.-N. Wang (Eds.), Quark–Gluon Plasma 3, World Scientific, Singapore, 2004, p. 634.
[21] A.K. Chaudhuri, arXiv:0801.3180 [nucl-th].
[22] D. Kharzeev, K. Tuchin, JHEP 0809 (2008) 093, arXiv:0705.4280 [hep-ph].
[23] F. Karsch, D. Kharzeev, K. Tuchin, Phys. Lett. B 663 (2008) 217, arXiv:0711.0914 [hep-ph].
[24] A. Monnai, T. Hirano, arXiv:0903.4436 [nucl-th].